

Metal-insulator transition and antiferromagnetic order in bis(ethylenedithio)tetrathiafulvalene tetracyanoquinodimethane (BEDT-TTF)(TCNQ)

Y. Iwasa, K. Mizuhashi, and T. Koda

Department of Applied Physics, University of Tokyo, Tokyo 113, Japan

Y. Tokura

Department of Physics, University of Tokyo, Tokyo 113, Japan

G. Saito

Department of Chemistry, Kyoto University, Kyoto 606, Japan

(Received 14 May 1993)

Electrical and magnetic properties have been investigated for (BEDT-TTF)(TCNQ) which is composed of BEDT-TTF sheets and TCNQ columns. The metal-insulator transition temperature T_{MI} , 330 K at ambient pressure, decreases down to 40 K by applying hydrostatic pressure, which may be ascribed to the change in both the intermolecular transfer energy and the band filling (molecular valence). Measurements of EPR and magnetic susceptibility indicate that the low-temperature states of BEDT-TTF sheets and TCNQ columns are magnetic insulators, perhaps due to strong electron correlation. An anomalous broadening of EPR linewidth observed below 35 K at ambient pressure suggests an occurrence of magnetic order in BEDT-TTF sheets. A subsequent antiferromagnetic order of TCNQ columns has been found at $T_N = 3.0 \pm 0.1$ K from the anisotropic magnetic susceptibility.

Development in the design and synthesis of (BEDT-TTF)-based organic metals has yielded more than 20 superconductors, and the highest T_c has now reached 13 K.¹ A characteristic feature of this family is the existence of two-dimensional (2D) conducting sheets of BEDT-TTF. In the meantime, a breakthrough was made in the research of the organic metals by the finding of magneto-oscillatory resistivity.^{2,3} The band picture based on the extended Hückel molecular orbitals appears to work well in the metallic BEDT-TTF sheets. However, there exist a large number of BEDT-TTF salts showing insulating behaviors or metal-insulator (MI) transitions, in spite that the band calculation predicts a metallic state for these materials. These insulating states or metal-insulator transitions in 2D BEDT-TTF salts have scarcely been explored in detail. Recent discovery of weak ferromagnetism in (BEDT-TTF)₂Cu[N(CN)₂]Cl (Ref. 4) shows that "high- T_c " superconductivity exists close to the magnetic insulator.

Up to now, most of studies have been made on the one-organic component salts with inorganic counterions (X), such as (BEDT-TTF)₂ X . Here, we report on transport and magnetic properties of a two-component system (BEDT-TTF)(TCNQ) to clarify the insulating state of the BEDT-TTF sheets and TCNQ columns. In the two-component system, the filling of the conduction band of BEDT-TTF sheets may be controlled by the mixed valent nature of the acceptor molecules. In fact, it is known that the band filling (nominal molecular valence) changes under high pressure in TTF-TCNQ.⁵ As is well known, the control of the band filling in oxides have revealed many novel properties of strongly correlated electron systems.⁶

Two different types of crystal structures are known for (BEDT-TTF)(TCNQ). The monoclinic phase has a mixed-stack column structure with low conductivity,⁷ while the triclinic form investigated here consists of 2D BEDT-TTF sheets and one-dimensional (1D) TCNQ columns⁸ as schematically depicted in the inset of Fig. 1. Precise structural analysis shows that both BEDT-TTF and TCNQ molecules are present in the form of dimer.⁸ Although the band calculation predicts a metallic state in (BEDT-TTF)(TCNQ), it undergoes an MI transition at $T_{MI} = 330$ K at ambient pressure.⁸

Let us start with an overview of the metal-insulator phenomena in (BEDT-TTF)(TCNQ) under pressure. Single crystals (typically $0.2 \times 0.5 \times 3$ mm³ in size) of triclinic (BEDT-TTF)(TCNQ) were grown by a direct reaction of 1,1,2-trichloroethane solutions of the component molecules. For the transport measurements, electrical contacts were made by gold paint. The crystal was loaded in a high-pressure clump cell that was cooled down to liquid He temperature. The temperature dependence of the resistivity along the elongated c axis (parallel to the TCNQ columns) is shown for various pressures in Fig. 1. The MI transition occurs at 330 K at ambient pressure in accord with the feature reported previously.⁸ By applying pressure, the resistivity rapidly decreases and the metallic state is maintained down to low temperatures. Below 40 K, the crystal does not show a metallic behavior, while the resistivity at 5 K decreases markedly with increasing pressure. The resistivity in the metallic state is considerably larger than the Mott limit (~ 6.5 m Ω cm, which is calculated for the 2D case) even at low temperatures. The anisotropy of the resistivity was also measured at ambient pressure at various temperatures as

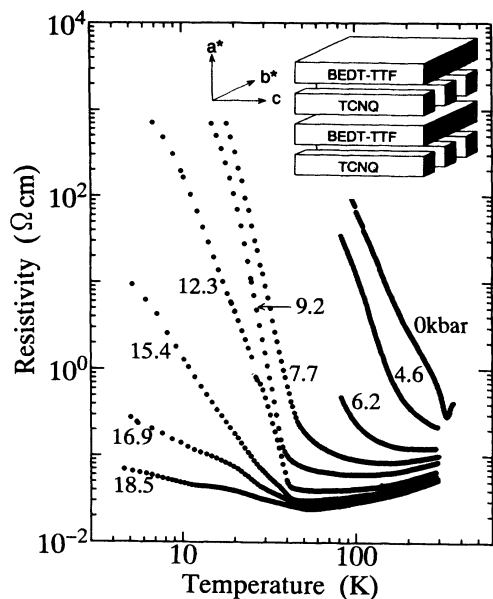


FIG. 1. Temperature dependence of resistivity of (BEDT-TTF)(TCNQ) for various pressures. A schematic crystal structure is shown in the inset.

well as under various pressures at room temperature. Both measurements show that the resistivity along the b^* axis (perpendicular to TCNQ columns) is only a few times larger than that along the c axis (parallel to the TCNQ columns), and imply that the BEDT-TTF sheets dominantly contribute to the metallic conduction.

In Fig. 2, we show a temperature-pressure diagram for the electronic phase in (BEDT-TTF)(TCNQ). T_{MI} is determined by the resistivity minimum. T_{MI} is remarkably reduced by application of pressure. Above 11 kbar, T_{MI} increases rather slightly with pressure. However, the low-temperature state below T_{MI} shows a crossover behavior from the localized to itinerant nature, as typically seen in a much reduced resistivity below T_{MI} at 18.5 kbar (Fig. 1).

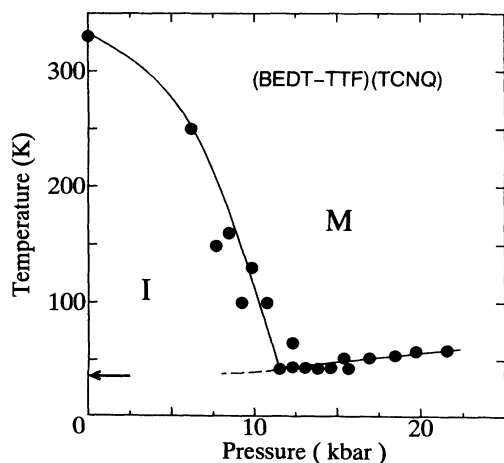


FIG. 2. Temperature-pressure phase diagram of (BEDT-TTF)(TCNQ). The solid lines are guides for eyes. The arrow indicates the temperature at which an anomaly in the EPR linewidth is observed.

To clarify the nature of the insulating state below T_{MI} in (BEDT-TTF)(TCNQ), we have carried out electron paramagnetic resonance (EPR) measurements in the temperature range between 5 and 330 K at ambient pressure. A small crystal of about $0.05 \times 0.2 \times 0.8 \text{ mm}^3$ was fixed on the quartz plate, which was sealed in a 5-mm-diam quartz tube with He gas. although (BEDT-TTF)(TCNQ) contains two spin-carrying components, i.e., BEDT-TTF sheets and TCNQ columns, only one EPR absorption signal of the Lorentzianlike shape was observed at all temperatures. This is attributed to the exchange narrowing effect that is commonly observed in two-component charge-transfer compounds such as TTF-TCNQ.⁹ In such a case, the averaged g value is expressed as¹⁰

$$\bar{g}(T) = \{\bar{g}_B \chi_B(T) + \bar{g}_Q \chi_Q(T)\} / [\chi_B(T) + \chi_Q(T)]. \quad (1)$$

Here, \bar{g}_B and \bar{g}_Q are the averaged g values of (BEDT-TTF)⁺ and TCNQ⁻ radicals, which are known to be $\bar{g}_Q = 2.0026$ and $\bar{g}_B = 2.007$,¹¹ respectively. $\chi_B(T)$ and $\chi_Q(T)$ are the individual spin susceptibility component of BEDT-TTF and TCNQ moieties.

The angle dependences of the g value and the peak-to-peak linewidth of the resonance curve have been measured by rotating the crystal around the two crystallographic axes (c and b^*). The two-axis rotation measurement could give the full g tensor, from which the averaged g value (\bar{g}) has been derived. Thus obtained \bar{g} value is plotted against temperature in Fig. 3(a). At 330 K, the $\bar{g} = 2.00424$ and is close to the mean value of \bar{g}_Q and \bar{g}_B . It decreases rapidly as the temperature is lowered. These results indicate that both BEDT-TTF and TCNQ radicals contribute to the spin susceptibility at high temperatures, while the relative contribution from BEDT-TTF is reduced at low temperatures. Figure 3(b) shows a temperature dependence of the peak-to-peak linewidth. It decreases with temperature down to 35 K due to the in-

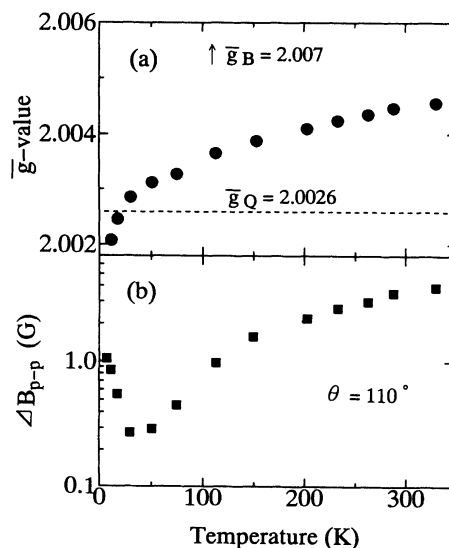


FIG. 3. Temperature dependence of the averaged g value (a) and the peak-to-peak linewidth ΔB_{p-p} (b). θ is the angle of the static magnetic field in the a^*b^* plane measured from the a^* axis. Similar behaviors are observed for other field directions.

crease of spin-lattice relaxation time, but shows a sharp upturn at around 35 K. This point is marked by an arrow in the T - P phase diagram (Fig. 2). Such a remarkable broadening of the EPR linewidth signals the presence of the internal magnetic field, implying the onset of magnetic ordering at around 35 K. This ordering is perhaps due to the spins on BEDT-TTF sheets, since the magnetic transition of the TCNQ spin system is observed at lower temperature as discussed later.

Magnetic dc susceptibility of the compound was measured to lower temperature (2 K) using a superconducting quantum interference device (SQUID) magnetometer. A contribution of the core diamagnetism, -2.67×10^{-4} emu/mol BEDT-TTF and -1.14×10^{-4} emu/mol TCNQ, have been subtracted from the raw data. Total spin susceptibility $\chi(T)$ is plotted against temperature in Fig. 4 by filled squares. No anomaly is observed at T_{MI} , and the $\chi(T)$ obeys the Curie-law below 100 K with the Curie constant of 3.0×10^{-4} emu K/g. The nominal spin density is estimated to be roughly one per four molecules [two units of (BEDT-TTF)(TCNQ)]. This result indicates that the observed MI transition differs from the Peierls transition, which causes the nonmagnetic ground state and is commonly observed in 1D charge-transfer compounds such as TTF-TCNQ.⁹

Using the relation (1), the total spin susceptibility $\chi(T) = \chi_B(T) + \chi_Q(T)$ can be decomposed into each contribution of BEDT-TTF and TCNQ. Here, averaged g values of individual components are assumed to be temperature independent. In fact, constant \bar{g} values are often observed for other BEDT-TTF compounds, where no magnetic phase transition occurs.¹² The decomposition procedure in the two-component organic compounds was applied first to the case of TTF-TCNQ,¹⁰ and its appropriateness was ensured by the NMR measurements.¹³ Figure 4 shows the data for χ_B and χ_Q , which are determined by the above-mentioned analysis. It is to be noted

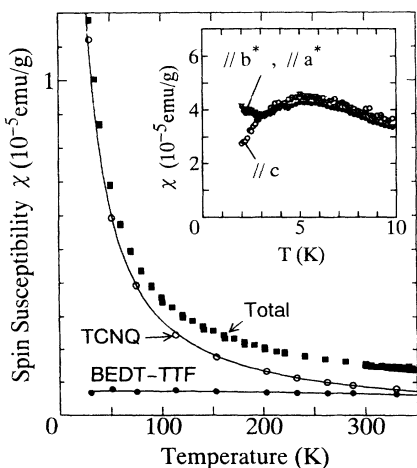


FIG. 4. Total spin susceptibility and individual contributions from the BEDT-TTF sheets and TCNQ columns. They are shown by solid squares, solid circles, and open circles, respectively. Solid lines are guides for eyes. The inset shows the low-temperature total susceptibility as a function of temperature for three field directions.

that the temperature dependence of $\chi_B(T)$ and $\chi_Q(T)$ is considerably different. [Below 35 K, we cannot apply the relation (1), since the internal field, which broadens the EPR linewidth, also affects the apparent \bar{g} values.] The susceptibility χ_B of the BEDT-TTF sheets is relatively small and does not strongly depend on temperature even in the insulating phase ($T < T_{MI}$), while $\chi_Q(T)$ for the TCNQ columns is Curielike as a whole. These results suggest that the spins in the BEDT-TTF sheets are subject to a strong antiferromagnetic coupling or otherwise verge on the itinerant state. Similar behavior and magnitude of χ is also observed in other 2D BEDT-TTF salts (BEDT-TTF)₂X, where $X^- = \text{Cu}[\text{N}(\text{CN})_2]\text{Cl}^-$, ICl_2^- , IClBr^- , or AuBr_2^- .¹⁴

As is clearly seen in Fig. 4, the Curielike magnetic susceptibility of (BEDT-TTF)(TCNQ) is dominated by the contribution from TCNQ columns. Therefore, the estimated spin density from the Curie constant (one per four molecules) corresponds to one spin per one TCNQ dimer. This implies that the degree of charge transfer from donor (BEDT-TTF) to acceptor (TCNQ) is $\sim \frac{1}{2}$ and all the electronic bands for BEDT-TTF and TCNQ are nearly one quarter filled. Due to the dimerization of the BEDT-TTF and TCNQ sites, however, the conduction band splits into two,⁸ even in the case of no electron correlation, so that the upper conduction band originating from HOMO (the highest occupied molecular orbital) of BEDT-TTF and LUMO (the lowest occupied molecular orbital) of TCNQ can be, respectively, viewed as half filled. This is also the case for (BEDT-TTF)₂X-type metallic salts. In insulating (BEDT-TTF)(TCNQ), however, the intradimer Coulomb interaction (corresponding to the Hubbard U term) may further split the upper conduction band into the lower and upper Hubbard bands, and the charge freedom is frozen out. In this view, the BEDT-TTF sheets are 2D Mott-Hubbard insulators.

At lower temperatures below 10 K, we have observed a deviation of the total susceptibility $\chi(T)$ from the Curie law. In the inset of Fig. 4, the anisotropy of χ is shown in the low-temperature region. We have observed a broad maximum of $\chi(T)$ at 5 K and a subsequent sharp onset of anisotropy in $\chi(T)$ at 3.0 ± 0.1 K. $\chi(\parallel c)$ decreases, while the $\chi(\parallel a^*$ or $\parallel b^*)$ increases as the temperature is lowered. These features are characteristic of an antiferromagnetic ordering of the Heisenberg spin systems at the Néel temperature $T_N = 3.0$ K. Since the low-temperature susceptibility was found to be dominated by TCNQ spins as shown in Fig. 4, we can conclude that the TCNQ columns undergo an antiferromagnetic transition at T_N . This is the first observation of magnetic ordering of spin systems on TCNQ columns. The ground states of the TCNQ columns in organic compounds is mostly nonmagnetic (spin singlet) due to the lattice instabilities such as Peierls or spin-Peierls mechanisms.¹⁵ We suggest that the magnetic interaction between TCNQ columns are mediated by intervening magnetic BEDT-TTF sheets and result in the antiferromagnetic order.

Keeping in mind these features of the insulating phase at ambient pressure, let us go back to the phase diagram (Fig. 2). In Fig. 2 the MI phase boundary above 11 kbar looks to be extrapolated to the point indicated by the ar-

row, at which the EPR linewidth shows the anomalous broadening at ambient pressure. Therefore, the MI phase boundary above 11 kbar is possibly related to the magnetic ordering of BEDT-TTF spins. Qualitatively similar features have been observed in doping- or pressure-induced changes of the electronic states of Mott-Hubbard systems, such as V_2O_3 (Ref. 16) and $LaTiO_3$ (Ref. 17). Incidentally, a unified phase diagram has been presented for quasi-1D organic tetramethyltetrafulvalene (TMTTF) family¹⁸ as a function of transfer energy (t). In this case, the low- t insulating phase is the nonmagnetic spin-Peierls phase due to its quasi-1D nature. In sharp contrast, the 2D nature of the insulating BEDT-TTF sheets in

(BEDT-TTF)(TCNQ) makes its ground state magnetic, and even the TCNQ columns undergoes the antiferromagnetic transition perhaps via intercolumn magnetic interaction.

The authors are grateful to M. Kinoshita and M. Tamura for their experimental help in the EPR measurements and enlightening discussion. They also thank S. Uchida and H. Eisaki for their help in the SQUID measurements. This work was supported in part by Grant-in-Aids for Scientific Research from Ministry of Education, Science and Culture, Japan.

¹J. M. Williams *et al.*, *Science* **252**, 1501 (1991).

²K. Oshima, T. Mori, H. Inokuchi, H. Urayama, H. Yamochi, and G. Saito, *Phys. Rev. B* **38**, 938 (1988).

³M. W. Kartsovnik *et al.*, *Pis'ma Zh. Eksp. Teor. Fiz.* **48**, 498 (1988) [*JETP Lett.* **48**, 541 (1988)]; K. Kajita *et al.*, *Solid State Commun.* **70**, 1189 (1989).

⁴U. Welp *et al.*, *Phys. Rev. Lett.* **69**, 840 (1992).

⁵A. Andrieux *et al.*, *Phys. Rev. Lett.* **43**, 227 (1979); S. Megtert *et al.*, *Solid State Commun.* **31**, 977 (1979).

⁶For an example, see *Physica (Amsterdam)* **185-189C** (1991).

⁷T. Mori and H. Inokuchi, *Bull. Chem. Soc. Jpn.* **60**, 402 (1987).

⁸T. Mori and H. Inokuchi, *Solid State Commun.* **59**, 355 (1986).

⁹Y. Tomkiewicz, E. M. Engler, and T. D. Shultz, *Phys. Rev. Lett.* **35**, 456 (1975).

¹⁰Y. Tomkiewicz, A. R. Taranko, and J. B. Torrance, *Phys. Rev. Lett.* **36**, 751 (1976).

¹¹T. Sugano, G. Saito, and M. Kinoshita, *Phys. Rev. B* **34**, 117 (1986).

¹²H. Urayama *et al.*, *Synth. Met.* **27**, A393 (1988).

¹³E. R. Rybaczewski, L. S. Smith, A. F. Garito, A. J. Heeger, and B. G. Silbernagel, *Phys. Rev. B* **14**, 2746 (1976).

¹⁴M. Tokumoto *et al.*, *Synth. Met.* **19**, 215 (1987).

¹⁵J. B. Torrance, in *Low Dimensional Conductors and Superconductors*, NATO Advanced Study Institutes, Series B, Vol. 155, edited by D. Jérôme and L. G. Caron (Plenum, New York, 1987), p. 113.

¹⁶S. A. Carter, T. F. Rosenbaum, J. M. Honig, and J. Spalek, *Phys. Rev. Lett.* **67**, 3440 (1991).

¹⁷Y. Okada, T. Arima, Y. Tokura, C. Murayama, and N. Mōri, *Phys. Rev. B* **48**, 9677 (1993).

¹⁸D. Jérôme, *Science* **252**, 1509 (1991).

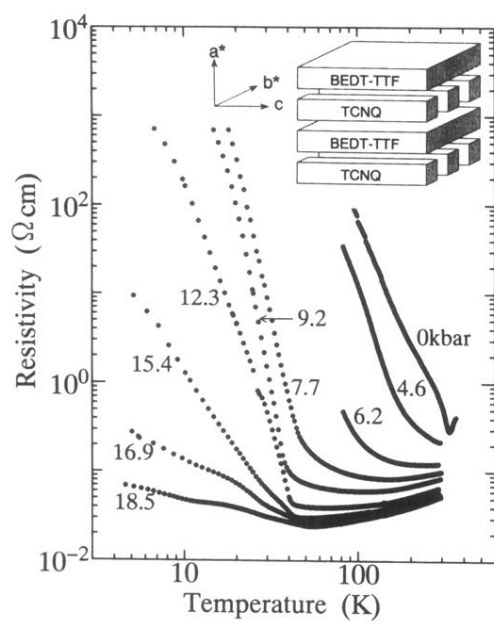


FIG. 1. Temperature dependence of resistivity of (BEDT-TTF)(TCNQ) for various pressures. A schematic crystal structure is shown in the inset.